ARTICLE

Journal of Materials Chemistry
www.rsc.org/materials

Synthesis, structural, and magnetic characterization of substituted benzoimidazole-l-yl *N*,*N*′-dioxides

Alexander Zakrassov,[a] Vitaly Shteiman,[a] Yana Sheynin,[a] Boris Tumanskii,[a] Mark Botoshansky,[a] Moshe Kapon,[a] Amit Keren,[b] Menahem Kaftory,*[a] Thomas E. Vos[c] and Joel S. Miller[c]

[a]*Department of Chemistry and Lise Meitner Minerva Center for the Computational and Quantum Chemistry, Technion - Israel Institute of Technology, Haifa 32000, Israel. E-mail: kaftory@tx.technion.ac.il; Fax: (972)-48295703; Tel: (972)-48233761*
[b]*Department of Physics, Technion - Israel Institute of Technology, Haifa 32000, Israel*
[c]*Department of Chemistry, University of Utah, Salt Lake City, UT 84112-0850, USA*

Received 9th January 2004, Accepted 5th April 2004
First published as an Advance Article on the web 13th May 2004

The crystal structures, EPR spectra and magnetic properties of the novel halogen- and cyano-substituted nitronyl nitroxide radicals 2-(2,6-dichlorophenyl)benzimidazolyl *N*,*N*′-dioxide, **6**, 2-(2,6-difluorophenyl)benzimidazolyl *N*,*N*′-dioxide, **7**, 2-(2-chloro-6-fluorophenyl)benzimidazolyl *N*,*N*′-dioxide, **8**, 2-(2,3,6-trichlorophenyl)benzimidazolyl *N*,*N*′-dioxide, **9**, 2-(2,3,4,5,6-pentafluorophenyl)benzimidazolyl *N*,*N*′-dioxide, **10**, and 2-(3-cyanophenyl)benzimidazolyl *N*,*N*′-dioxide, **11**, are reported. Compound **6** crystallizes in the triclinic crystal system in space group $P\bar{1}$. The molecules of **6** are arranged in pairs with short intermolecular distances between the NO groups. **7** crystallizes in two different modifications: polymorph α is orthorhombic, space group *Pbca*; polymorph β is monoclinic, space group $P2_1/c$. **8** crystallizes in two modifications: the α polymorph is monoclinic, space group $P2_1/c$; and the β polymorph is monoclinic, space group $P2_1/n$. **9** crystallizes in the monoclinic system, space group $P2_1/c$. **10** crystallizes in the monoclinic system, space group $C2/c$. The molecules of **10** are packed in pairs of two types that form a chain perpendicular to the *c*-axis. **11** crystallizes in the monoclinic crystal system in space group $P2_1/c$. The rotation angle between the two rings in compounds **6**–**10** is 54.2–76.7°. The rotation angle between the two rings is only 21.0° in **11** and it strongly affects the packing of the molecules that adopt the stacking mode. The magnetic measurements show that **6**, **7**, **10** and **11** exhibit large magnetic coupling. The best fitting with the experimental data for **6** and **11** was obtained using the Bleaney–Bowers singlet–triplet model plus the Curie–Weiss spin impurity ($S = 1/2$; $H = -2J\,S_1 \cdot S_2$) $J/k_B = -84.2$ K and $\theta_{imp} = 0.3$ K and $J/k_B = -95.3$ K, $\theta_{imp} = 1.8$ K, respectively. A Pade expression for **7** revealed $J_{intra}/k_B = 66.0$ K and $zJ_{inter}/k_B = -14.0$ K. Compound **10** shows evidence for large antiferromagnetic spin coupling ($\theta = -37.0$ K Curie–Weiss model).

Introduction

The quest for organic materials exhibiting technologically useful properties, such as electric conductivity or ferromagnetism, started several decades ago. The goal was to create an assembly of organic molecules or macromolecules made up from only light elements (C, H, N, O, S, *etc.*) and yet possessing properties similar to those of pure metals to conduct electricity by electron mobility or some metals to enable spin alignment. The possibility of ferromagnetic coupling in organic radicals was theoretically predicted in 1963 by McConnell.[1] The first example of an organic bulk ferromagnet was reported in 1991 by Kinoshita and co-workers for-the β-*p*-nitrophenyl nitronyl nitroxide radical (**1**, R=PhNO$_2$).[2] The evidence for the existence of long-range ferromagnetic order for this compound was achieved by *ac* susceptibility and heat-capacity measurements at low temperatures. The ferromagnetic behavior was detected at 0.60 K (T_c). It is interesting to note that the α- and γ-phases did not show ferromagnetic ordering, indicating that it is not sufficient to have a stable organic radical, and that magnetism is a bulk property and therefore highly dependent upon the solid-state structure.[3]

Since 1991, there has been a tremendous effort of many research groups worldwide to identify mechanisms to achieve stabilized ferromagnetic ordering. The belief that even the most sophisticated properties can be rationally designed by a systematic modification of organic molecular structures is motivated and fuelled by increased synthetic capabilities, especially for obtaining large organic molecules with suitable structures and topologies, and also by the spectacular progress of supramolecular chemistry for materials development witnessed in recent years. In this quest, stable organic radicals such as **2** and **3** that are ordered as ferromagnets were prepared.[4,5] However, the goal of easily preparing compounds that will show ferromagnetic properties at ambient temperatures is yet beyond reach.

Ferro- or antiferro-magnetic coupling of stable radicals depends upon the spin density on each atom and the interactions between them.[6] Since no correlation was found between the relative orientation of O–N=C–N–O$^{\bullet}$ groups and the types of coupling,[7,8] it appears that ferro- or antiferro-magnetic coupling in the nitronyl nitroxide radicals is dependent upon the shortest contacts between all the atoms (*i.e.* hydrogen bonds and van der Waals interactions) and their spin densities.

In the past decade many substituted nitronyl nitroxide radicals related to **1** have been deliberately synthesized and their magnetic properties studied with the goal of identifying additional examples of magnetically ordered organic materials; this has met with limited success and has been without identification of a material that has a higher T_c than **1**.[7,8] Herein, we report the synthesis and study of the magnetic properties of several substituted benzoimidazole-l-yl *N*,*N*′-dioxides, **4**. This is a class of nitronyl nitroxides that has not been studied in detail.

Replacing the saturated –Me$_2$CCMe$_2$– backbone with a fused

DOI: 10.1039/b400299g

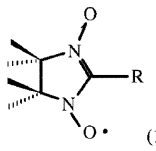

(1)

T_C = 0.60 K (for R = $PhNO_2$)

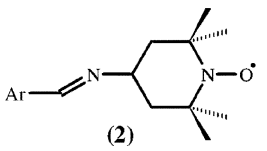

(2)

T_C = 0.1-0.4 K

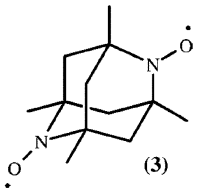

(3)

T_C = 1.48 K

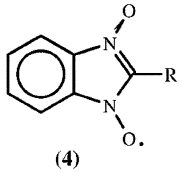

(4)

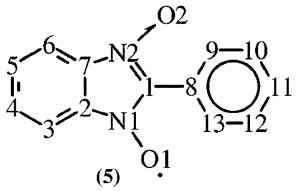

(5)

phenyl ring will control the packing and it is hoped to lead to shorter intermolecular contacts. However, the atomic spin densities on the NO groups are reduced due to the unpaired electron delocalizing onto the benzoimidazole ring and therefore the magnetic coupling should be reduced.[9] Nonetheless, the presence of spin on the fused aromatic ring provides an additional means of coupling between the radicals in three-dimensions in the solid that can lead to magnetic ordering. For example, the computed B3LYP with the 6–31 G(d) basis set spin distributions for **1** and **4** (R = H) reveal that each NO has 0.61 of the spin for **1** (R = H) and 0.55 of the spin for **4** (R = H) and the spin on the central C is −0.25 and −0.21 for **1** and **4** (R = H), respectively. The spin of the remaining carbons for **1** (R = H) is miniscule (0.02), but is 0.17 for **4** (R = H).

Phenylbenzoimidazole-l-yl *N*,*N*′-dioxide (PBIDO), **5**, is the only benzoimidazole nitroxide radical whose magnetic properties have been reported and it is the only benzoimidazole whose structure is known.[10] Compound **5** dimerizes and exhibits strong antiferromagnetic coupling. The magnetic properties of these stable radicals, which can be a building block for new advanced magnetic materials, need to be explored.

In the present work we describe and discuss the structures of eight crystals of six new benzoimidazole nitroxide radicals (two of them crystallize in two polymorphic forms), as well as the EPR spectra and magnetic properties of four of them: 2-(2,6-dichlorophenyl)benzimidazolyl *N*,*N*′-dioxide (**6**), 2-(2,6-difluorophenyl)benzimidazolyl *N*,*N*′-dioxide (**7**), 2-(2,3,4,5,6-pentafluorophenyl)benzimidazolyl *N*,*N*′-dioxide (**10**) and 2-(3-cyanophenyl)benzimidazolyl *N*,*N*′-dioxide (**11**).

Results and discussion

Crystal structures

Molecular packing in the unit cells is given in supplementary material. Molecular structures and atomic numbering are given in Fig. 1. Comparison of selected bond lengths and angles in the nitronyl nitroxide moiety of the six compounds **6**–**11** is given in Table 1. Atomic notations are given in Fig. 1. The intramolecular bond lengths and angles of **6**–**11** are very similar to those observed for the reference compound **5**.[10] Moreover, the α-polymorph of 2-(2,6-difluorophenyl)benzimidazolyl *N*,*N*′-dioxide, **7**, and **5** are isostructural.

The conformation of the molecules may be compared by the rotation angle between the benzimidazolyldioxide and the substituted phenyl ring. The rotation angle is determined by the size of the substituent in the *ortho* position of the phenyl ring. Therefore it is 66.1(4)° in the compound possessing 2,6-dichlorophenyl, **6**, and 54.2(5) and 54.6(4)° in the two polymorphs of the compound possessing 2,6-difluoropenyl, **7**. The rotation angle in the compound possessing 2,3,4,5,6-pentafluorophenyl, **10**, is 58.8(3)° and this angle is 76.7(4)° in the compound possessing 2,3,6-trichlorophenyl, **9**. In the absence of a substituent in the *ortho* position, such as in **11** and **5**, the rotation angles are 21.0(3) and 10.0° respectively.

2-(2,6-Dichlorophenyl)benzimidazolyl *N*,*N*′-dioxide, **6**, crystallizes in the triclinic crystal system in space group $P\bar{1}$. The molecules of **6** are arranged in stacks along the *a*-axis. Molecules within a stack are paired through face-to-face contacts of

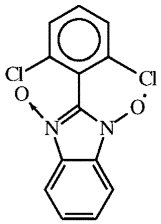

(6)

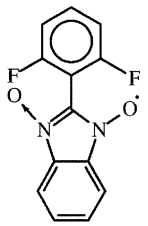

(7)

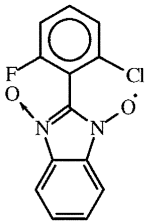

(8)

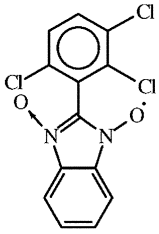

(9)

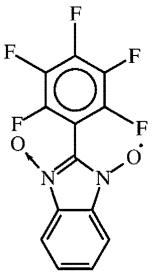

(10)

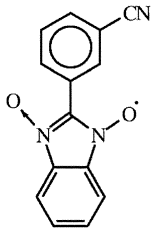

(11)

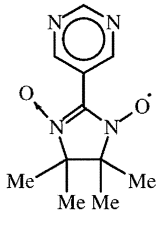

(12)

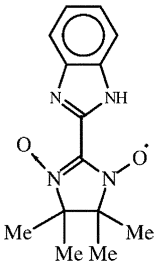

(13)

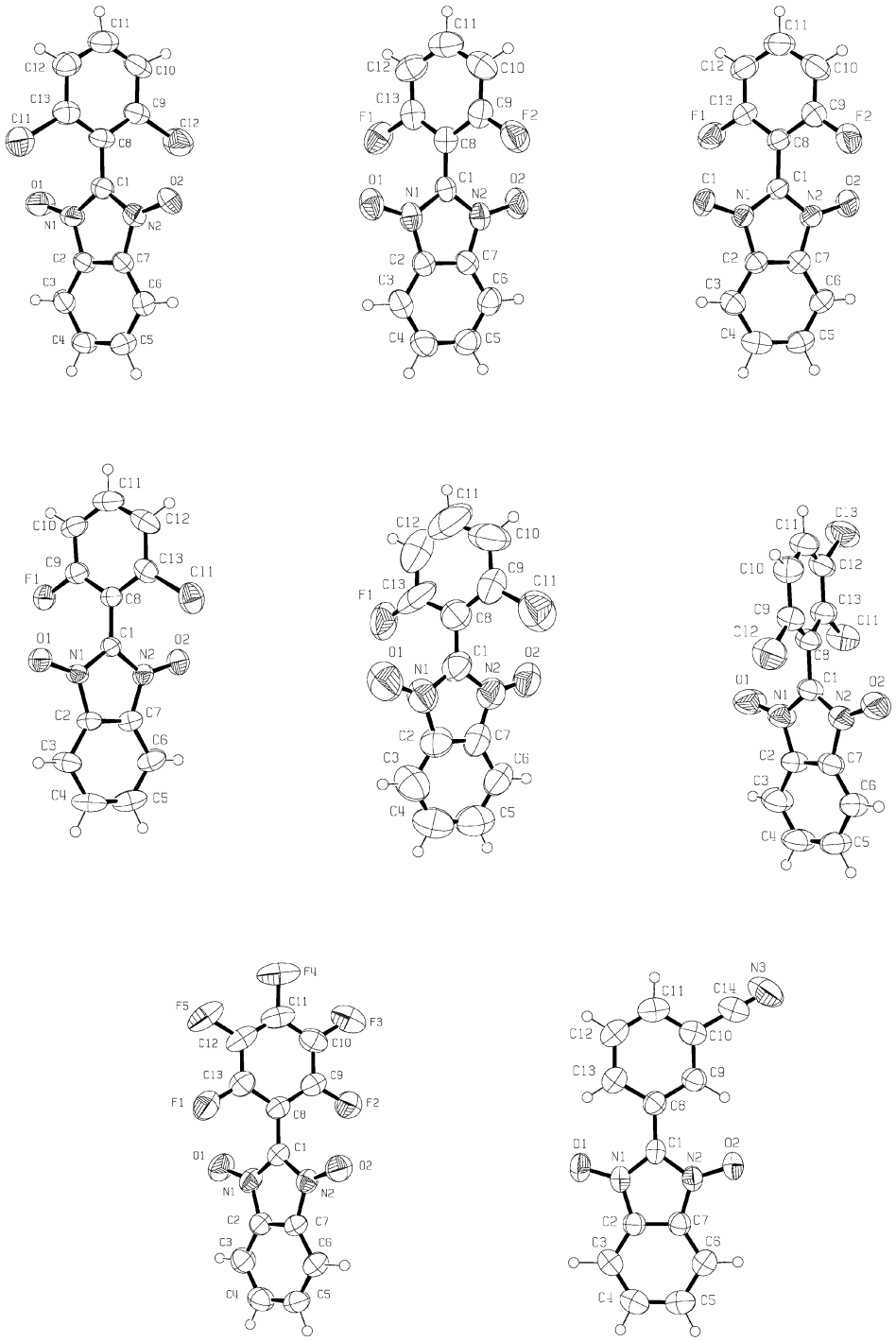

Fig. 1 Molecular structures and atomic numbering. Top left to right: **6**, **7**α, **7**β; middle left to right: **8**α, **8**β, **9**; bottom left to right: **10**, **11**.

the benzimidazolyldioxide rings. Parallel stacks are held by interactions between parallel phenyl rings.

2-(2,6-Difluorophenyl)benzimidazolyl *N*,*N*′-dioxide, **7**, crystallizes in two polymorphic forms. The α-polymorph crystallizes in the orthorhombic crystal system in space group *Pbca*. The molecules of **7**α are arranged in pairs with parallel benzimidazolyldioxide rings running perpendicular to the *b*-axis. The β-polymorph crystallizes in the monoclinic crystal system in space group $P2_1/c$. The molecules are packed in stacks with molecular pairing through parallel benzimidazolyldioxide rings.

2-(2-Chloro-6-fluorophenyl)benzimidazolyl *N*,*N*′-dioxide, **8**, crystallizes in two polymorphic forms. The α-polymorph crystallizes in the monoclinic crystal system in space group $P2_1/c$. The β-polymorph crystallizes in the monoclinic crystal system in space group $P2_1/n$.

2-(2,3,6-Trichlorophenyl)benzimidazolyl *N*,*N*′-dioxide, **9**, crystallizes in the monoclinic crystal system in space group $P2_1/c$.

2-(2,3,4,5,6-Pentafluorophenyl)benzimidazolyl-*N*,*N*′-dioxide, **10**, crystallizes in the monoclinic crystal system in space group *C*2/*c*. The structure of **10** is made up by two types of pairs of molecules that form a chain perpendicular to the *c*-axis. There are short interpair contacts F1···F2 3.116(3) Å, F3···F4 2.835(3) Å, F5···O2 3.158(3) Å and F5···C10 2.960(3) Å.

2-(3-Cyanophenyl)benzimidazolyl *N*,*N*′-dioxide, **11**, crystallizes in the monoclinic crystal system in space group $P2_1/c$. The molecule is significantly planar compared with the halogen-substituted compounds **6**–**10** as expressed by the torsion angle of 21.0(2)° between the cyanophenyl and the benzimidazolyl moieties. The molecules adopt the stacking packing mode. Layers of molecules perpendicular to the *c*-axis form parallel

Table 1 Bond lengths (Å) angles (°), and the rotation angles between the two rings in **6**–**11**

	6	**7α**	**7β**	**8α**	**9**	**10**	**11**	**5**[10]
O(1)–N(1)	1.270(3)	1.277(3)	1.277(3)	1.274(4)	1.271(3)	1.276(2)	1.284(3)	1.279
O(2)–N(2)	1.270(4)	1.278(3)	1.280(3)	1.265(4)	1.277(3)	1.267(2)	1.284(3)	1.275
N(1)–C(1)	1.366(5)	1.357(4)	1.368(4)	1.354(5)	1.348(4)	1.351(3)	1.362(3)	1.364
N(1)–C(2)	1.426(4)	1.415(4)	1.412(4)	1.418(5)	1.419(4)	1.409(3)	1.414(3)	1.413
N(2)–C(1)	1.369(4)	1.369(4)	1.355(4)	1.374(5)	1.355(4)	1.361(3)	1.370(3)	1.373
N(2)–C(7)	1.369(4)	1.369(4)	1.355(4)	1.374(5)	1.355(4)	1.415(3)	1.370(3)	1.373
C(1)–C(8)	1.455(5)	1.441(4)	1.447(4)	1.450(6)	1.460(4)	1.447(3)	1.447(4)	1.453
C(2)–C(7)	1.373(5)	1.382(4)	1.372(4)	1.370(6)	1.362(4)	1.375(3)	1.373(4)	1.373
O(1)–N(1)–C(1)	126.2(3)	126.8(3)	126.3(3)	126.1(3)	125.4(3)	126.1(2)	126.6(2)	127.1
O(1)–N(1)–C(2)	124.8(3)	123.3(3)	125.0(3)	124.9(3)	125.1(3)	124.5(2)	123.5(2)	122.8
C(1)–N(1)–C(2)	108.9(3)	109.9(3)	108.6(3)	109.0(3)	109.4(3)	109.4(2)	109.9(2)	110.1
O(2)–N(2)–C(1)	126.1(3)	126.6(3)	125.8(3)	126.5(4)	127.5(3)	126.4(2)	126.9(2)	127.5
O(2)–N(2)–C(7)	125.3(3)	124.7(3)	124.7(3)	124.8(4)	124.2(3)	125.1(2)	123.4(2)	122.7
C(1)–N(2)–C(7)	108.6(3)	108.7(3)	109.5(3)	108.7(3)	109.2(3)	108.5(2)	109.7(2)	109.8
N(1)–C(1)–N(2)	108.1(3)	107.8(3)	107.8(3)	107.9(3)	107.8(3)	108.2(2)	106.7(2)	106.4
N(1)–C(1)–C(8)	126.9(3)	126.6(4)	125.8(3)	125.7(3)	126.9(3)	125.8(2)	126.9(3)	126.8
N(2)–C(1)–C(8)	125.0(4)	125.5(3)	126.4(3)	126.4(3)	125.2(3)	126.0(3)	126.4(2)	126.8
C(7)–C(2)–N(1)	106.9(3)	106.4(3)	107.6(3)	107.3(4)	106.9(3)	106.8(2)	106.7(2)	106.8
C(2)–C(7)–N(2)	107.5(3)	107.2(4)	106.5(3)	107.0(4)	106.7(3)	107.1(2)	107.0(2)	106.9
Rotation angle	66.1(4)	54.6(4)	54.2(5)	62.0(6)	76.7(4)	58.8(3)	21.0(3)	10.0

stacks with the nitrogen atoms of the cyano groups as the borders between the stacks.

The understanding of the relation between the magnetic properties and the three-dimensional structural motif is important for further development in the field. The spin couplings, J, are determined from fitting the temperature-dependent susceptibility, χ, $\chi(T)$ to different models. Structurally one may distinguish between four different types of intermolecular interactions based on O···O distances. The upper limit for the O···O distance was set to 4.0 Å. In 2-(2,3,6-trichlorophenyl)-benzimidazolyl *N*,*N*′-dioxide, **9**, there are no short contacts between oxygen atoms and therefore no strong interactions between spins are expected. In the second type of structure, molecules are arranged in dimers distant from other dimers. This type was observed for **6**, **8**α, and **8**β (Fig. 2), where the intermolecular O···O distances are 3.048(4), 3.005(5), and 2.917(8) Å, respectively. In the third structural type the molecules are arranged in infinite chains. In **7**α, **7**β, and **5** (Fig. 3), the chains are made up by short contacts between the oxygen atoms. However, while in **7**β, and **9** the distances are not equivalent [2.996(2) and 3.958(5) Å, and 3.083(3) and 3.841(3) Å, respectively], these distances are equivalent [3.414(3) Å] in **7**α. The fourth structural motif was observed in 2-(3-cyanophenyl)benzimidazolyl *N*,*N*′-dioxide, **11**. The O···O interactions are two-dimensional (Fig. 4) and the intermolecular O···O distances ranged from 3.178(3) to 3.224(3) Å.

EPR spectra

The high-resolution EPR spectra of **6**, **7**, **10**, and **11** are characterized by the hyperfine coupling of the unpaired electron with two equivalent ^{14}N nuclei (I = 1) and aromatic protons (I = 1/2) in the benzoimidazole ring. The g-factors for **6**, **7**, **10** and **11** were found to be 2.0068 ± 0.0003. The experimental and B1LYP with the 6-31G(d) basis-set-calculated nitrogen (a_N) and hydrogen (a_H) hyperfine coupling constants (hfccs) are summarized in the Table 2. The experimental a_N for **5** was reported to be 4.38 G.[11]

The spectra of **7** and **10** exhibit the additional hyperfine splitting (Fig. 5) caused by the presence of fluorine nuclei (I = 1/2) at the 2,6-positions in the phenyl ring (a_F = 0.18 G for **7** and **10**) and hydrogen (fluorine) nuclei at the *para* positions (a_H = 0.18 G for **7** and a_F = 0.36 G for **5**). Similar hfccs were obtained for **11** (a_H = 0.30 G at the *para* position and a_H = 0.20 G at the 2,5,6-positions).

The experimental a_N and a_H as well as the calculated spin densities for the present radicals show that unpaired electron delocalization only slightly depends upon the molecular geometries and on the substituents. The a_N and a_H for the different halogen-substituted nitronyl nitroxide radicals containing the

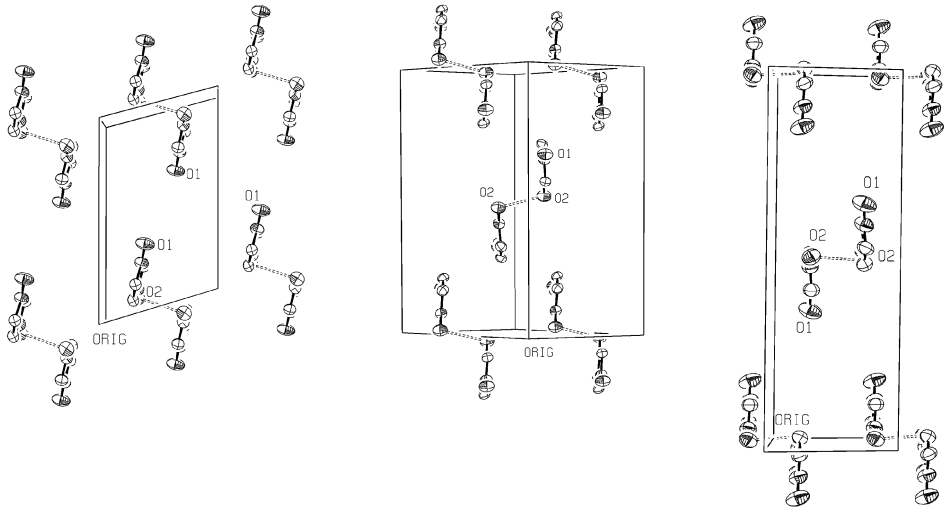

Fig. 2 Geometry of the intermolecular O···O interactions forming dimers in **6** (left), **8**α (center), and **8**β (right).

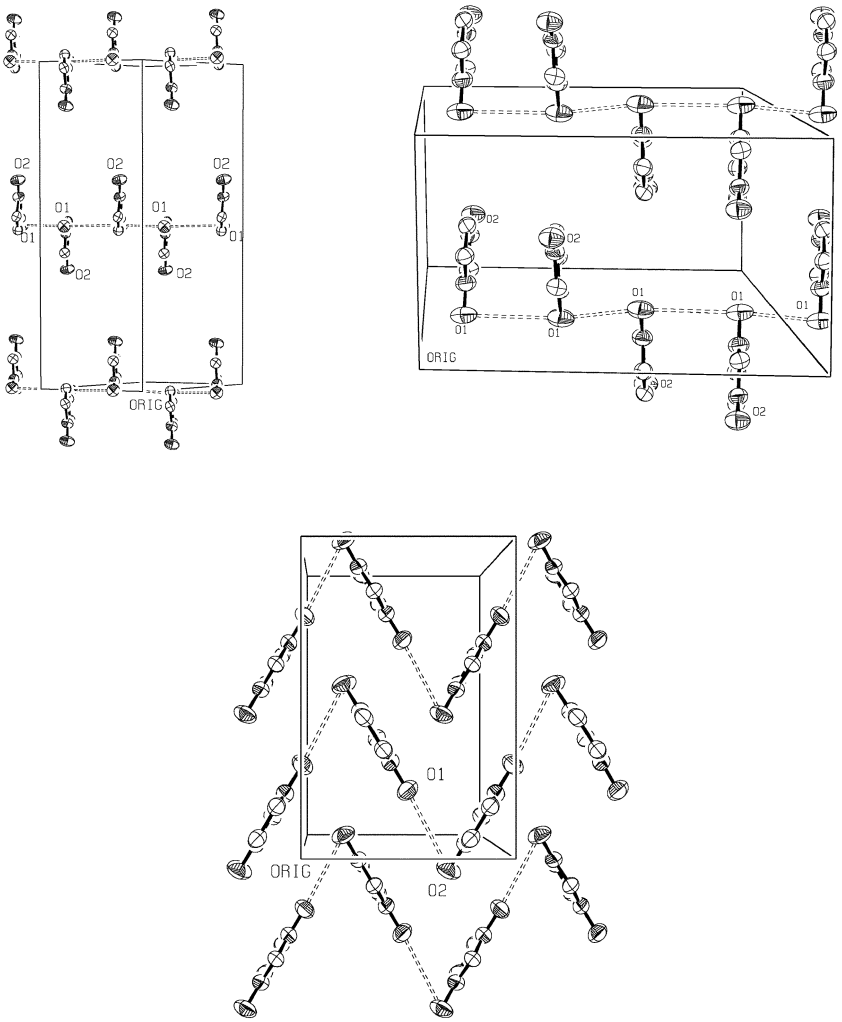

Fig. 3 Geometry of the intermolecular O···O interactions forming chains in **7**β (top left), **10** (top right), and **7**α (bottom). The intermolecular O···O distances are 2.996(2) and 3.958(5) Å in **7**β, 3.083(3) and 3.841(3) Å in **10**, and 3.414(3) in **7**α.

saturated –Me_2CCMe_2– backbone, **1**, where R = Ph, have been reported to be 7.2–7.8 and 0.24–0.60 G (in the *ortho* position), 0.30–0.49 G (in the *para* position), 0.12–0.25 G (in the *meta* position) and 0.18–0.21 G (–Me_2CCMe_2– backbone), respectively.[12] The smaller a_N and the larger a_H of the benzoimidazole ring suggest larger unpaired electron delocalization on the benzoimidazole carbons in comparison with the methyl carbons of **1**. The smaller spin densities on NO and the larger spin densities on the benzoimidazole carbons calculated by B3LYP with the 6-31G(d) basis set also support the same results.[9]

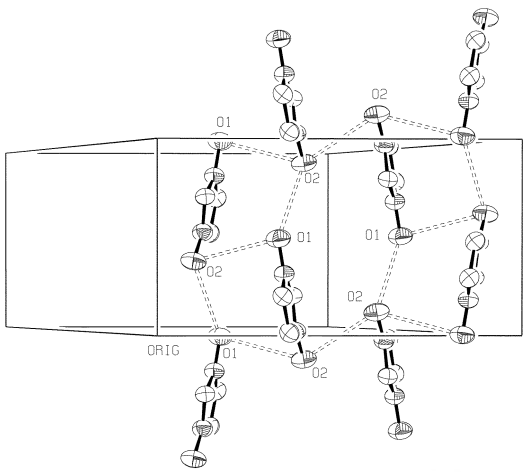

Fig. 4 Structure of **11** exhibiting two-dimensional O···O interactions. The intermolecular O···O distances are 3.178(3)–3.224(3) Å.

Magnetic data

The molar magnetic susceptibility, χ, between 2 and 300 K was measured for **6**, **7**, **10**, and **11** (Table 3; Fig. 6). The effective moments, μ_{eff} [$\equiv(8\chi T)^{1/2}$], at 300 K of **6**, **7**, **10**, and **11** were 1.55, 1.52, 1.51, and 1.28 μ_B, respectively. The effective moments of **6**, **7**, **10** and **11** were reduced from the expected value of 1.73 μ_B for an S = 1/2 spin, indicative of antiferromagnetic coupling.[13]

In each case the moment remains relatively constant with

Table 2 Nitrogen (a_N) and hydrogen (a_H) isotropic hyperfine coupling constants (G) for **6**, **7**, **10**, **11**

	a_N		a_H		
Compound	Exp.	Calc.	Exp.	Calc.	
6	4.09	3.93	0.84	0.80	0.95[a]
7α	4.10	3.91	0.71	0.81	0.97[a]
10	4.07	3.75	0.71	0.77	0.96[a]
11	4.11	4.20	0.70	0.80	1.04[a]

[a] For the protons at the 2,5-positions in the benzoimidazole ring.

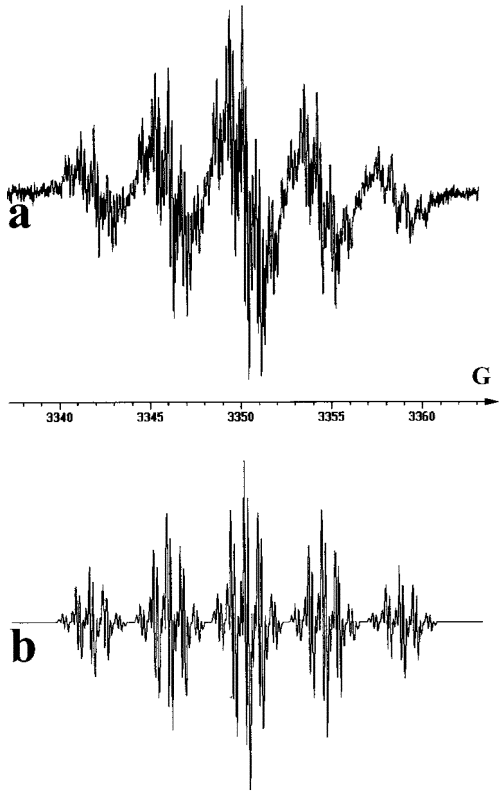

Table 3 Summary of the magnetic data for **6**, **7**, **10** and **11**

Compound	f^a	J/k_B (K)	zJ'/k_B (K)	μ_{eff} at 300 K (μ_B)	θ (K)
6	0.96	-84.2^b	—	1.55	−72.1
7α	0.71	66.0^c	-14^c	1.52	31.2
10	0.96	-37.0^d	—	1.52	−37.0
11	0.65	-95.3^b	—	1.28	−83.9

[a] f is a scaling factor to account for the purity of the radical. [b] The J/k_B value was obtained from the Bleaney–Bowers model. [c] The coupling between spins was obtained from a Pade linear chain model. [d] −37.0 K is the Weiss constant (θ) from the Curie–Weiss model.

decreasing temperature until approximately 200 K (Fig. 6) when it decreases for **6**, **10**, and **11**, indicative of antiferromagnetic coupling, but increases for **7** in accord with ferromagnetic coupling.

The spin couplings, J, of **6**, **7**, **10**, and **11** were determined from fitting the magnetic data to different magnetic models appropriate to each structure along with the Curie–Weiss model [shown later in eqn. (6)] in the high temperature regime for each radical (Table 3). In accord with the dimerized structure for **6** in the crystal structure, $\chi(T)$ for **6** was fit to S = 1/2 with the Bleaney–Bowers model[14] [eqn. (1), where μ_B is the Bohr magneton, N = Avrogadro's number, k_B = Boltzmann's constant, and g is the Lande g-factor], with a Curie–Weiss S = 1/2 spin impurity, P_{imp}, along with a purity factor f,[15] and $H = -2\,J\,S_1 \cdot S_2$. The presence of an S = 1/2 spin impurity is typically observed and is attributed to crystal defects.

$$\chi_{dimer} = f\frac{Ng^2\mu_B^2}{k_B T}\frac{1}{3+e^{2x}};\ x=\frac{J}{k_B T};$$
$$\chi_{total} = \chi_{dimer} + P_{imp}\frac{C}{T-\theta_{imp}};\ C=\frac{Ng^2\mu_B^2}{k_B} \quad (1)$$

The best-fit parameters obtained were J/k_B = −84.2 K, f = 0.96, P_{imp} = 0.0085, and θ_{imp} = 0 K. The relatively large J/k_B = −84.2 K indicated a strong antiferromagnetic coupling (Fig. 6). This is comparable to that observed for

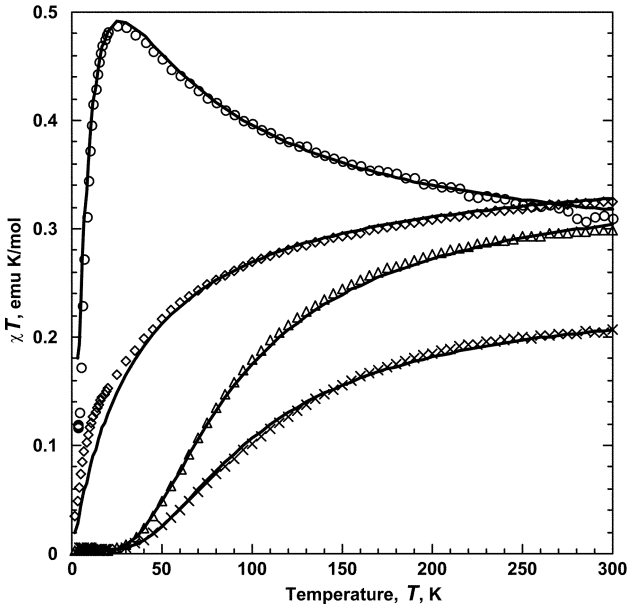

Fig. 6 $\chi T(T)$ for 2,6-Dichloro nitronyl nitroxide **6** (△), 2,6-difluoro nitronyl nitroxide **7** (○), 2,3,4,5,6-pentafluoro nitronyl nitroxide **10** (◇), and 3-cyano nitronyl nitroxide **11** (×). The solid curves were calculated with the parameters reported in the text.

2-imidazole-4,4,5,5-tetramethylimidazoline N,N'-dioxide with J/k_B = −89 K,[16] and is significantly greater than that observed for **5** with J/k_B = −38 K indicating that benzoimidazol-l-yl N,N'-dioxides can couple strongly.[10]

2,6-Difluoro nitronyl nitroxide, **7**, has been isolated as a mixture of the two polymorphs, **7**α with a small amount of **7**β. **7**α has a linear chain with O···O intrachain contacts of 3.414 Å and the interchain O···O contacts of 5.415, 6.064 and 6.261 Å; it has three nearest neighbors (z = 3) (Fig. 3, bottom). In contrast, **7**β may be described as an alternating chain with O···O intrachain contacts of 2.996 and 3.958 Å and the interchain O···O contacts of 5.284, 5.908 and 6.950 Å (Fig. 3, top left). The magnetic data of **7** were fit to three uniform chain models: the Bonner–Fisher (BF) [eqn. (2)],[17] Pade [eqn. (3)],[18] and Hatfield [eqn. (4)][19] models since the crystal structure of **7**α showed a linear chain structure. The Bonner–Fisher model [eqn. (2)] describes a Heisenberg spin system of antiferromagnetically coupled uniformly spaced spins. While eqn. (2) applies only to anitferromagnetically coupled spins, the Pade expression [eqn. (3)] expands the equation to account for either anitferromagnetically or ferromagnetically coupling between uniformly spaced spins. The Hatfield expression [eqn. (4)] extends to an alternating linear chain model to bridge the gap between a dimer and linear chain model for antiferromagnetically coupled spins by including alternating coupling constants J and σJ.[19] At σ = 1, the Hatfield expression describes a uniformly spaced linear spin chain, and at the other limit of σ = 0, the Hatfield model describes a spin dimer. Each of these models included a purity factor f component and a Curie–Weiss spin impurity component P_{imp}.[15]

$$\chi_{Ch1} = f\frac{Ng^2\mu_B^2}{k_B T}\frac{0.25+0.14995x+0.30094x^2}{1+1.9862x+0.68854x^2+6.0626x^3};$$
$$x=\frac{|J|}{k_B T};\ J\le 0 \quad (2)$$

$$\chi_{Ch2} = f\frac{Ng^2\mu_B^2}{4k_B T}\left[\frac{1+0.57979916K+16.902653K^2+29.376885K^3+29.832959K^4+14.036918K^5}{1+2.7979916K+7.0086780K^2+8.6538644K^3+4.5743114K^4}\right]^{\frac{2}{3}};\quad (3)$$
$$K=\frac{J}{2k_B T}$$

$$\chi_{Ch3} = f\frac{Ng^2\mu_B^2}{k_B T}\frac{0.25 + 0.063465x + 0.0140763x^2}{1 + 0.687355x + 0.58384582x^2 + 0.179409x^3};$$
$$x = \frac{2|J|}{k_B T};\ \sigma = 1;\ J \le 0 \quad (4)$$

Using molecular field approximation to account for small magnetic coupling between chains, the total calculated magnetic susceptibility was provided by eqn. (5):[20]

$$\chi_i = \frac{\chi_{Chi}}{1 - (2zJ'/Ng^2\mu_B^2)\chi_{Chi}} + P_{imp}\frac{C}{T - \theta_{imp}};$$
$$C = \frac{Ng^2\mu_B^2}{k_B};\ J \gg zJ' \quad (5)$$

Fitting the magnetic susceptibility data of **7** with eqn. (2) and (4) resulted in poor correlation, whereas good agreement between experimental and calculated magnetic data was obtained with eqn. (3) (Fig. 6). The best-fit parameters of eqn. 3 were: $J/k_B = 66$ K, $zJ'/k_B = -14$ K, and $f = 0.71$. This indicates significant ferromagnetic coupling between spins within the chain, and a weaker antiferromagnetic coupling between chains. The magnetic impurity might result from decomposition of the radical **7** to its precursor **7H** as well as from the presence of the second polymorph, **7**β, that cannot be removed.

IR spectra of compounds **8** and **9** show significant C–H stretches indicating the presence of hydrocarbon impurities. Moreover, **8** crystallizes in two polymorphs that could not be separated. Therefore the magnetic properties of the two compounds were not measured.

The crystal structure of pentafluoro nitronyl nitroxide (**10**) may be described as an alternating chain with O···O intrachain contacts of 3.083(3) and 3.841(3) Å and the interchain O···O contacts of 5.261(3), 6.414(3) and 6.706(3) Å (Fig. 5, $z = 3$). While the Hatfield expression, eqn. (4), would appear to be an ideal choice of model for the magnetic behavior of **5**, a satisfactorily fit, however, could not be obtained. The $\chi(T)$ could not be satisfactorily fitted with the Bonner–Fisher [eqn. (2)], Pade [eqn. (3)], or Bleaney–Bowers [eqn. (1)] expressions. In order to quantify the coupling between the nitroxide spins, the $\chi(T)$ was satisfactorily fit using the Curie–Weiss model in a high temperature regime (above 60 K in this case) [eqn. (6)], (Fig. 6). The majority of magnetic susceptibilities with complicated coupling mechanisms are able to be modeled with the Curie–Weiss expression in a high temperature regime.

$$\chi_i = f\frac{C}{T - \theta};\ C = \frac{Ng^2\mu_B^2}{k_B} \quad (6)$$

The best-fit parameters were $\theta = -37.0$ K and $f = 0.96$, indicating significant antiferromagnetic coupling between independent spins and the presence of a 4% diamagnetic impurity.

The crystal structure of 3-cyano nitronyl nitroxide (**11**) shows a linear chain with O···O intrachain contacts of 3.178(3) Å and short interchain O···O contacts between each molecule of 3.207(3) and 3.224(3) (twice) Å (Fig. 4). The two-dimensional interactions between the spins are complicated and the magnetic susceptibility was fitted with the Bonner–Fisher [eqn. (2)], Pade [eqn. (3)], and Hatfield expression [eqn. (4)] linear chain models and a 2-D square-planar model [eqn. (7)];[21] however, they unsatisfactorily describe the experimental data.

$$\chi = f\frac{Ng^2\mu_B^2}{4\kappa_B T}\frac{1}{1 + 2x + 2x^2 + 1.333x^3 + 0.25x^4 - 0.4833x^5 + 0.003797x^6};$$
$$x = \frac{|J|}{k_B T};\ J \le 0 \quad (7)$$

The magnetic susceptibility data, however, could be fitted with a Bleaney–Bowers, dinuclear spin model with $J/k_B = -95.3$ K, $f = 0.65$, $P_{imp} = 0.010$, and $\theta_{imp} = 1.8$ K. This fit indicates that the material contained approximately 35% of a diamagnetic impurity, *e.g.* **11H** (Fig. 6). While the magnetic coupling between nitroxides appears complicated due to their structure, the observed coupling is in accord with a simple dinuclear spin model. Further research is being carried out to understand which coupling pathways dominate and account for these magnetic data.

The interpretation of the presence of 35% of diamagnetic **11H** is perplexing as although the ν_{C-N} IR stretching band for **11H** and **11** differ by an easily detectable 4 cm^{-1}, the IR spectrum contains only one ν_{C-N} absorption. Powder X-ray diffraction was performed on the material used for the magnetic studies and the data perfectly matched the expected pattern calculated from the crystal structure, therefore providing no evidence of a secondary crystal phase which might account for the observed magnetic data. Mass spectrometry of **11H** had a parent ion peak at 251.0 amu whereas the mass spectrometry of the oxidized product of **11H**, **11**, had a parent ion peak at 250.0 amu. Thus, evidence that **11H** is not present; nonetheless, some unknown diamagnetic material must be present.

The magnetic behavior of substituted benzoimidazol-l-yl *N*,*N*′-dioxide radicals, **4**, has been shown to exhibit both ferro- and antiferro-magnetic coupling which has been modeled with Bleaney–Bowers, Curie–Weiss, or 1-D linear expressions [eqn. (1)–(6)].[10,12–19,22] Strong antiferromagnetic coupling obtained from a fit with the Bleaney–Bowers model was found for 2-imidazole-4,4,5,5-tetramethylimidazoline *N*,*N*′-dioxide with $J/k_B = -89$ K, and for **5** with $J/k_B = -38$ K.[10,16] Similarly, we found strong antiferromagnetic coupling for **6** with $J/k_B = -84.2$ K and **11** with $J/k_B = -95.3$ K. Similar to compound **7**, the magnetic data for 2-(5-pyrimidinyl)-4,4,5,5-tetramethylimidazoline *N*,*N*′-dioxide (**12**) and 2-(benzimidazol-2-yl)-tetramethylimidazoline *N*,*N*′-dioxide (**13**) were modeled with eqn. (3).[16,23] Both **12** and **13** had intermediate ferromagnetic coupling, *i.e.* $J/k_B = 26$ K for **12**, and weak antiferromagnetic coupling, *i.e.* $zJ/k_B = -4$ K for **12**, analogous to the magnetic behavior of **7**.

In the simple Heitler–London model the exchange coupling J is defined as a sum of the antiferro- ($2\beta S$) and ferro-magnetic (K) contributions with the opposite signs eqn. (8):

$$J = 2\beta S + K \quad (8)$$

where S and β are the overlap and resonance integrals, respectively, and K is the two-electron exchange integral.[24] In general, $2\beta S$ dominates. Ferromagnetic coupling is obtained when the overlap integral vanishes, *i.e.* two singly occupied molecular orbitals (SOMOs) are orthogonal.

Direct interaction of adjacent N–O groups cannot account for the ferromagnetic coupling in **12** or **7**α since the two SOMOs are far from orthogonal. Antiferromagnetic coupling, however, would be expected to be weak since the planes of O1–N1–C1–N2–O2 (the plane of the SOMO, Fig. 7) of two adjacent molecules are far from parallel (61.8°), and therefore the orbital overlap of the two SOMOs would be small. Similar to **7**α, Rey and co-workers could not explain the ferromagnetic coupling in **12** by direct inter-nitroxyl interactions (the angle between the planes of O1–N1–C1–N2–O2 of two adjacent molecules is 49.8°),[23] but rationalized the ferromagnetic coupling of **12** by using the McConnell model to explain the interaction of N–O···C1 as being a ferromagnetic coupling pathway.[1] According to the McConnell model pertaining to conjugated π radicals, the interaction of two groups with spin densities of opposite sign, *i.e.* N–O···C1, is a pathway for ferromagnetic coupling.

The calculation of the exchange coupling constant using the

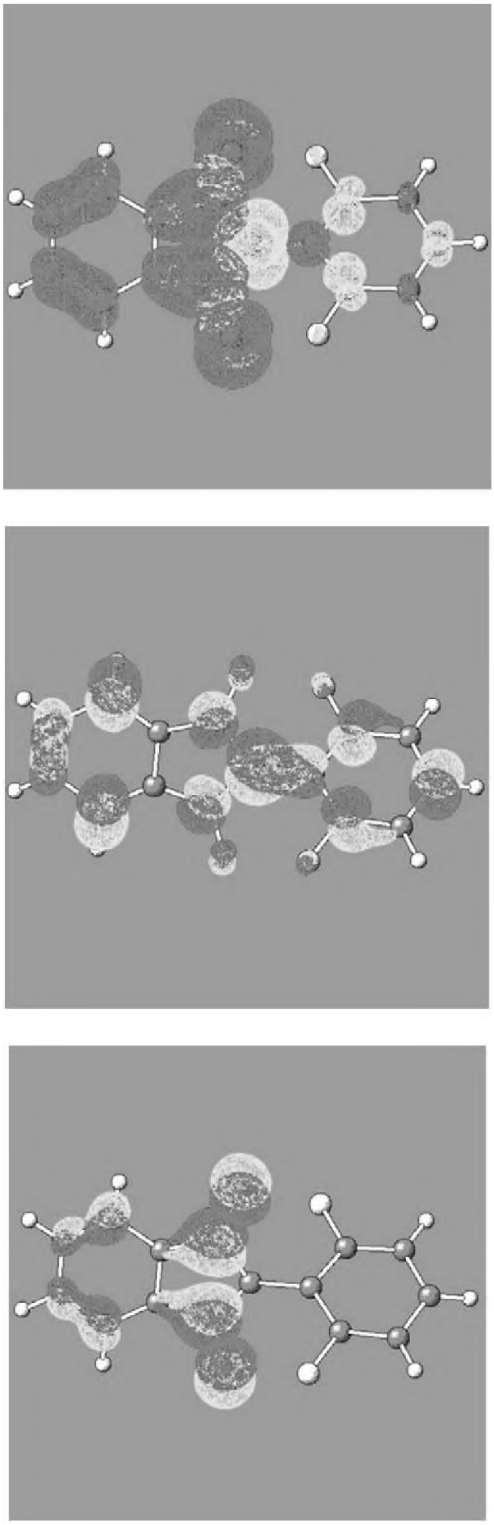

Fig. 7 B3LYP/6-31G(d) calculated spin densities (top), LUMO (center) and SOMO (bottom) for **7α** (gray is positive, white is negative).

McConnell model leads to an equation similar to eqn. (8) but with the inversion of the signs; $2\beta S$ becomes a ferromagnetic contribution, *i.e.* ferromagnetic coupling is obtained when the SOMO–LUMO are parallel.[1,24]

In **7α**, the N–O···C1 interaction would account for the observed ferromagnetic coupling since the distance between the groups is short (3.030 Å) and the angle between the O1–N1–C1–N2–O2 planes of adjacent nitronyl nitroxide molecules (61.8°) ensures a significant overlap.

5 and **7α** are isostructural (the angle between the planes of O1–N1–C1–N2–O2 of two adjacent molecules is 74.3° for **5**), but **5** exhibits an antiferromagnetic coupling. Considering SOMO–LUMO interactions between the O1–N1–C1–N2–O2 groups it is possible to explain the antiferromagnetic coupling of **5** and ferromagnetic coupling of **7α**. The LUMO lies within the C1–C8–C9–C13 plane (Fig. 7). The SOMO and LUMO of adjacent molecules in **7α** are almost parallel (8.1°) whereas for **5** the angle between the SOMO and the LUMO is 64.1°, which explains the ferromagnetic coupling of **7α**.

The N1–O1···C1 contact of **12** is shorter (2.92 Å), but the SOMO–LUMO angle of **12** is 30.5°, therefore the ferromagnetic coupling of **12** is smaller than that of **7α**. While this McConnell model qualitatively explains the ferromagnetic coupling in **7α**, the validity of this model has recently been questioned due to a lack of systematic correlation between the magnetic behavior and the three-dimensional crystal packing.[7,8] The correlation between the structure and the magnetic behaviors for **6**, **7**, **10**, and **11**, although explained by the O···O and N–O···C1 pathways, appears to be much more complicated than outlined above and needs further investigation.

Conclusions

Replacing the methyl shielding groups in the nitronyl nitroxide radicals with benzoimidazole leads to shorter intermolecular contacts between the NO groups (except in **4**). The molecules of the present radicals are arranged in both dimers (**6**, **8α**, **8β**) and infinite chains (**7α**, **7β**, **10**). Moreover, **11** exhibits very unusual 2-D N···O contacts. The present radicals can be a prospective building block for the new molecule-based organometallic magnetic materials. Preparation of the organometallic complexes on the basis of the present compounds is in progress.

Experimental

1. Syntheses

Compounds **6**–**11** were prepared by the following procedure. A solution of 2 mmol (276 mg) *o*-benzoquinone dioxime and 2 mmol of the corresponding aldehyde in 20 mL of ethanol and 0.8 mL of 8 mmol perchloric acid was stirred at 80 °C for 2 h.[25] After cooling to room temperature, 40 mL of water was added and the reaction mixture was neutralized with aqueous ammonia. The precipitate was washed with water and dried. The oxidation of 1-hydroxy-2-phenylbenzimidazole *N*-oxide (with the corresponding substituents) was carried out using an excess of PbO_2 in CH_2Cl_2. To a suspension of 1-hydroxy-2-phenylbenzimidazole *N*-oxide (with the corresponding substituents) in 50 mL of CH_2Cl_2, 12 g of powdered PbO_2 was added and stirred for 10 min to yield a green solution.[10] The residual mixture was filtered off and put into another 50 mL of CH_2Cl_2 followed by stirring for 10 min. The calculated yields are: **6**, 16%; **7**, 18%; **8**, 12%; **9**, 17%; **10**, 12%; and **11**, 19%.

2. X-Ray crystallography

Crystals suitable for X-ray-diffraction studies were obtained by slow evaporation of the reaction solvent. The diffraction intensity measurements for compounds **6**–**11** were carried out on a Nonius KappaCCD diffractometer with graphite monochromated MoKα radiation (λ = 0.71073 Å). Unit-cell parameters were determined from all the data.

Structure solutions and full-matrix, least squares refinements were accomplished with the SHELXS-97 PC package of programs.[26] All non-H-atoms were refined anisotropically. Hydrogen atoms were isotropically refined. Crystal data and further data-collection parameters for the studied compounds

Table 4 Crystallographic data and parameters for **6–11**

	6	**7α**	**7β**	**8α**	**8β**	**9**	**10**	**11**
Formula	$C_{13}H_7Cl_2N_2O_2$	$C_{13}H_7F_2N_2O_2$	$C_{13}H_7F_2N_2O_2$	$C_{13}H_7ClFN_2O_2$	$C_{13}H_7ClFN_2O_2$	$C_{13}H_6Cl_3N_2O_2$	$C_{13}H_4F_5N_2O_2$	$C_{14}H_8N_3O_2$
M	294.11	261.21	261.21	277.66	277.66	328.55	315.18	250.23
Crystal color, habit	Black, prism	Blue-green, prism	Black, prism	Black, prism	Black, prism	Black, prism	Dark brown, prism	Dark green, prism
Crystal dimensions/mm	0.12 × 0.06 × 0.01	0.30 × 0.06 × 0.01	0.12 × 0.12 × 0.03	0.42 × 0.06 × 0.03	0.20 × 0.12 × 0.05	0.12 × 0.12 × 0.06	0.15 × 0.10 × 0.08	0.12 × 0.09 × 0.06
Crystal system	Triclinic	Orthorhombic	Monoclinic	Monoclinic	Monoclinic	Monoclinic	Monoclinic	Monoclinic
Space group	$P\bar{1}$	*Pbca*	$P2_1/c$	$P2_1/c$	$P2_1/n$	$P2_1/c$	$C2/c$	$P2_1/c$
a/Å	7.580(1)	11.803(2)	6.942(1)	10.370(2)	7.396(1)	8.470(1)	22.536(5)	13.722(1)
b/Å	8.003(2)	7.833(1)	21.265(3)	15.787(3)	20.665(3)	12.701(2)	7.868(2)	7.138(2)
c/Å	11.652(2)	23.664(2)	8.886(1)	7.790(1)	8.180(1)	12.440(2)	13.760(2)	13.316(1)
α/°	88.60(2)	90.00	90.00	90.00	90.00	90.00	90.00	90.00
β/°	74.12(2)	90.00	121.30(2)	109.68(2)	105.38(2)	93.79(2)	100.69(2)	118.23(2)
γ/°	68.84(2)	90.00	90.00	90.00	90.00	90.00	90.00	90.00
V/Å^3	631.8(2)	2187(5)	1120.9(4)	1200.8(4)	1205.4(3)	1335.3(3)	2397.5(9)	1149.1(4)
Z	2	8	4	4	4	4	8	4
D_{calc}/g cm^{-3}	1.546	1.586	1.548	1.536	1.530	1.634	1.746	1.446
μ(MoKα)/cm^{-1}	0.051	0.013	0.013	0.033	0.033	0.069	0.017	0.010
F(000)	298	1064	1256	564	564	660	1256	516
2*θ* max/°	50.64	50.06	50.10	50.02	48.68	50.70	54.76	51.64
Reflections collected	6069	6317	2003	9048	1310	4437	4241	3277
Independent reflections	2218	1635	1972	2106	1310	2433	2373	1994
Observed reflections	1050	647	1005	1524	501	1156	1018	1019
Largest difference peak/e Å^{-3}	0.192	0.141	0.201	0.781	0.167	0.161	0.140	0.247
Largest difference hole/e Å^{-3}	−0.258	−0.162	−0.175	−0.434	−0.190	−0.181	−0.153	−0.360
No. of parameters	200	172	173	172	172	181	199	172
R^a	0.0503	0.0455	0.0493	0.0898	0.0608	0.0401	0.0421	0.0453
wR^a	0.0981	0.0710	0.1418	0.2320	0.1675	0.1055	0.1027	0.1020
GOF^b	0.899	0.819	0.977	1.075	0.848	0.825	0.815	0.926

^{a} $R = \Sigma||F_o| - |F_c||/\Sigma|F_o|$; $wR = [\Sigma w(|F_o| - |F_c|)^2/\Sigma w|F_o|^2]^{1/2}$. ^{b} GOF $= [\Sigma w(|F_o| - |F_c|)^2/(NO - NV)]^{1/2}$, where *NO* is the number of observations and *NV* is the number of variables.

are summarized in Table 4. Crystals of **8**β show poor diffraction and therefore the precision of the geometric parameters is low.

CCDC reference numbers 228541–228548. See http://www.rsc.org/suppdata/jm/b4/b400299g/ for crystallographic data in .cif or other electronic format.

3. EPR spectroscopy

X-Band (9.3 GHz) EPR spectra of **6**, **7**, **10** and **11** were obtained in toluene solution at room temperature on a Bruker EMX-10/12 spectrometer equipped with the variable-temperature accessory. A 100 kHz modulation frequency was used. The radical solution samples were carefully degassed by bubbling with the pure argon to avoid dipolar broadening resulting from the presence of atmospheric oxygen in the solutions. The SimFonia package was used for the simulations of the spectra and for refinement of the isotropic hyperfine coupling constants.

4. Magnetic measurements

Magnetic susceptibility measurements were made between 2 and 300 K using a Quantum Design MPMS-5 5T SQUID magnetometer with a sensitivity of 10^{-8} emu or 10^{-12} emu/Oe at 1 T and equipped with a reciprocating sample measurement system and continuous low-temperature control with enhanced thermometry features. All magnetic susceptibility measurements were made on powders contained in gel cap holders at 1000 Oe. The data were corrected for the diamagnetism calculated from standard diamagnetic susceptibility tables for each sample: -138×10^{-6} emu mol^{-1} for **6**, -117×10^{-6} emu mol^{-1} for **7**, -127×10^{-6} emu mol^{-1} for **10**, and -119×10^{-6} emu mol^{-1} for **11**. The magnetic susceptibility data for **7** were obtained for three independently made samples. The shape of the magnetic susceptibility was the same after accounting for the ferromagnetic impurity in one of the samples, but the room temperature moment varied from 1.43 to 1.52 μ_B. The highest room temperature moment sample was considered to be the purest sample. The magnetic susceptibility for **11** was obtained for three independently made samples. The shape of the magnetic data was the same for all three, but the room temperature moment varied from 1.08 to 1.28 μ_B.

5. IR spectroscopy

IR spectra were obtained from KBr pellets between 400 and 4000 cm^{-1} using a Bruker Tensor 37 spectrometer.

6. Mass spectrometry

Mass spectrometry measurements of **11** and **11**H were carried out on a Finnigan MAT95 instrument using the electron impact ionization (EI) method.

7. Powder XRD

Powder XRD data were obtained from a Rigaku X-Ray Diffraction System with CuKα radiation.

Acknowledgements

This research was supported by the United States-Israel Binational Science Foundation Grant No. 1997389, and by The Israel Science Foundation (ISF) (Grant No. 4001/03-50.0). Y. S. and B. T. gratefully acknowledge support provided by The Center for Absorption in Science, Ministry of Immigrant Absorption, state of Israel. T. E. V. and J. S. M. gratefully acknowledge support from the US NSF (Grant No. CHE 0110685) and US DOE (Grant No. DE-FG-93ER45504).

References

1 H. M. McConnell. *J. Chem. Phys.*, 1963, **39**, 1910.
2 M. Tamura, Y. Nakazava, K. Nozava, D. Shiomi, Y. Hosokushi, M. Ishikava, M. Takahashi and M. Kinoshita. *Chem. Phys. Lett.*, 1991, **186**, 401; P. Turek, K. Nozawa, D. Shiomi, K. Awaga, T. Inabe, Y. Maruyama and M. Kinoshita. *Chem. Phys. Lett.*, 1991, **180**, 327.
3 J. S. Miller. *Adv. Mater.*, 1998, **10**, 1553–1557.
4 T. Nogami, K. Tomioka, T. Ishida, H. Yoshikawa, M. Yasui, F. Iwasaki, H. Iwamura, N. Takeda and M. Ishikawa. *Chem. Lett.*, 1994, 29; K. Togashi, R. Imachi, K. Tomioka, H. Tsuboi, T. Ishida, T. Nogami, N. Takeda and M. Ishikawa. *Bull. Chem. Soc. Jpn.*, 1996, **69**, 2821 and refs. cited therein.
5 R. Chiarelli, A. Novak, A. Rassat and J. L. Tholence. *Nature*, 1993, **363**, 147.
6 J. S. Miller and A. J. Epstein. *Angew. Chem., Int. Ed. Engl.*, 1994, **33**, 385.
7 M. Deumal, J. Cirujeda, J. Veciana and J. J. Novoa. *Adv. Mater.*, 1998, **10**, 1461.
8 M. Deumal, J. Cirujeda, J. Veciana and J. J. Novoa. *Chem. Eur. J.*, 1999, **5**, 1631.
9 A. Zakrassov and M. Kaftory. *J. Solid. State. Chem.*, 2002, **169**, 75.
10 Y. Kusaba, M. Tamura, Y. Hosokoshi, M. Kinoshita, H. Sawa, R. Kato and H. Kobayashi. *J. Mater. Chem.*, 1997, **7**, 1377.
11 D. Shiomi, K. Sato, T. Takui, K. Itoh, M. Tamura, Y. Nishio, K. Kajita, M. Nakagawa, T. Ishida and T. Nogami. *Mol. Cryst. Liq. Cryst.*, 1999, **335**, 359.
12 O. Jurgens, J. Cirujeda, M. Mas, I. Mata, A. Cabrero, J. Vidal-Cancedo, C. Rovira, E. Molins and J. Veciana. *J. Mater. Chem.*, 1997, **7**, 1723; J. Cirujeda, J. Vidal-Gansedo, O. Jurgens, F. Mota, J. J. Novoa, C. Rovira and J. Veciana. *J. Am. Chem. Soc.*, 2000, **122**, 11393.
13 Values less than the calculated spin-only value of 1.73 μ_B are attributed to weighting errors, incomplete radical formation from the nitronyl nitroxide precursor, and antiferromagnetic coupling.
14 B. Bleaney and K. D. Bowers. *Proc. R. Soc. London, Ser. A*, 1952, 214.
15 The purity factor f was included to account for diamagnetic impurity in the product. See: T. Mitsumori, K. Inoue, N. Koga and H. Iwamura. *J. Am. Chem. Soc.*, 1995, **117**, 2467; T. Matsumoto, T. Ishida, N. Koga and H. Iwamura. *J. Am. Chem. Soc.*, 1992, **114**, 9952.
16 N. Yoshioka, M. Irisawa, Y. Mochizuki, T. Kano, H. Inoue and S. Ohba. *Chem. Lett.*, 1997, 251.
17 J. C. Bonner and M. E. Fisher. *Phys. Rev.*, 1964, **135**, A640.
18 G. A. Baker, G. S. Rushbrooke and H. E. Gilbert. *Phys. Rev.*, 1964, **135**, A1272.
19 J. W. Hall, W. E. Marsh, R. R. Weller and W. E. Hatfield. *Inorg. Chem.*, 1981, **20**, 1033.
20 O. Kahn. *Molecular Magnetism*. VCH Publishers, Inc. New York, 1993, pp. 26–29.
21 G. S. Rushbrooke and P. J. Wood. *Mol. Phys.*, 1958, **1**, 257; M. E. Lines. *J. Phys. Chem. Solids*, 1970, **31**, 101.
22 For recent nitronyl nitroxide papers, see: Y. Pei, O. Kahn, M. A. Abersold, L. Ouahab, F. Le Berre, L. Pardi and J.-L. Tholence. *Adv. Mater.*, 1994, **6**, 681; T. Sugawara, M. Matsushita, A. Izuoka, N. Wada, N. Takeda and M. Ishikawa. *J. Chem. Soc., Chem. Commun.*, 1994, 1723; K. Awaga, A. Yamaguchi, T. Okuno, T. Inabe, T. Nakamura, M. Matsumoto and Y. Maruyama. *J. Mater. Chem.*, 1994, **4**, 1377; A. Canneschi, F. Ferraro, D. Gatteschi, A. Le Lirzin, M. A. Novak, E. Rentschler and R. Sessoli. *Adv. Mater.*, 1995, **7**, 476; J. Cirujeda, E. Hernandez-Gasio, C. Rovira, J.-L. Stanger, P. Turek and J. Veciana. *J. Mater. Chem.*, 1995, **5**, 243; T. Mitsumori, K. Inoue, N. Koga and H. Iwamura. *J. Am. Chem. Soc.*, 1995, **117**, 2467; A. Lang, Y. Pei, L. Ouahab and O. Kahn. *Adv. Mater.*, 1996, **8**, 60; M. Matsushita, A. Izuoka, T. Sugawara, T. Kobayashi, N. Wada, N. Takeda and M. Ishikawa. *J. Am. Chem. Soc.*, 1997, **119**, 4369; R. Akabane, M. Tanaka, K. Matsuo and N. Koga. *J. Org. Chem.*, 1997, **62**, 8854; S. Nakatsuji and H. Anzai. *J. Mater. Chem.*, 1997, **7**, 2161; S. Nakatsuji, M. Saiga, N. Hage, A. Naito, T. Hirayana, M. Nakagawa, Y. Oda, H. Anzai, K. Suzuki, T. Enoki, M. Mito and K. Takeda. *New J. Chem.*, 1998, **22**, 275; M. Tanaka, K. Matsuda, T. Itoh and H. Iwamura. *J. Am. Chem. Soc.*, 1998, **120**, 7168; T. Otsuka, T. Okuno, K. Awaga and T. Inabe. *J. Mater. Chem.*, 1998, **8**, 1157; L. Catala, J. Le Moigne, N. Kyritsakas, P. Rey, J. J. Novoa and P. Turek. *Chem. Eur. J.*, 2001, **7**, 2467; N. Claiser, M. Souhassou, C. Lecomte, Y. Pontillon, F. Romero and R. Ziessel. *J. Phys. Chem. B*, 12896, **106**, 12.

23 F. Lanfranc de Panthou, D. Luneau, J. Laugier and P. Rey, *J. Am. Chem. Soc.*, 1993, **115**, 9095.
24 C. Kollmar and O. Kahn, *J. Chem. Phys.*, 1993, **98**, 453.
25 F. Patzold, H. J. Niclas and E. Grunedeman, *J. Prakt. Chem.*, 1990, **332**, 345.
26 G. M. Sheldrick, *SHELXS97, Program for the Solution of Crystal Structures*, University of Göttingen, Germany, 1997; G. M. Sheldrick, *SHELXL97, Program for the Refinement of Crystal Structures*, University of Göttingen, Germany, 1997.